

AD A047535

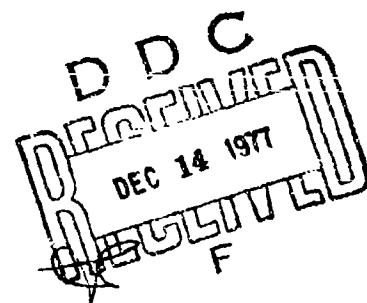
RADC-TR-77-243  
IN-HOUSE REPORT  
JULY 1977

12  
D.S.



## Detection of Targets in Noise and Clutter

RONALD L. FANTE



Approved for public release; distribution unlimited.

AD No. \_\_\_\_\_  
DDC FILE COPY

ROME AIR DEVELOPMENT CENTER  
AIR FORCE SYSTEMS COMMAND  
GRIFFISS AIR FORCE BASE, NEW YORK 13441

This report has been reviewed by the RADC Information Office (OI) and is releasable to the National Technical Information Service (NTIS). At NTIS it will be releasable to the general public, including foreign nations.

APPROVED:

*Walter Rotman*

WALTER ROTMAN

Chief, Microwave Detection Techniques Br.  
Electromagnetic Sciences Division

APPROVED:

*Allan C. Schell*

ALLAN C. SCHELL

Acting Chief

Electromagnetic Sciences Division

FOR THE COMMANDER:

*John P. Huns*

Plans Office

Unclassified

SECURITY CLASSIFICATION OF THIS PAGE (When Data Entered)

REPORT DOCUMENTATION PAGE		READ INSTRUCTIONS BEFORE COMPLETING FORM	
1. REPORT NUMBER RADC-TR-77-243	2. GOVT ACCESSION NO.	3. RECIPIENT'S CATALOG NUMBER	
4. TITLE (and Subtitle) DETECTION OF TARGETS IN NOISE AND CLUTTER		5. TYPE OF REPORT & PERIOD COVERED In-House	
7. AUTHOR(s) Ronald L./Fante		6. PERFORMING ORG. REPORT NUMBER	
9. PERFORMING ORGANIZATION NAME AND ADDRESS Deputy for Electronic Technology (RADC/ETEP) Hanscom AFB Massachusetts 01731		8. CONTRACT OR GRANT NUMBER(s)	
11. CONTROLLING OFFICE NAME AND ADDRESS Deputy for Electronic Technology (RADC/ETEP) Hanscom AFB Massachusetts 01731		10. PROGRAM ELEMENT, PROJECT, TASK APL A WORK UNIT NUMBERS 46001403 62702F 681900	
14. MONITORING AGENCY NAME & ADDRESS (if different from Controlling Office)		12. REPORT DATE Jul 77	
		13. NUMBER OF PAGES 40	
		15. SECURITY CLASS. (of this report) Unclassified	
16. DISTRIBUTION STATEMENT (of this Report) Approved for public release; distribution unlimited.		15a. DECLASSIFICATION/DOWNGRADING SCHEDULE	
17. DISTRIBUTION STATEMENT (of the abstract entered in Block 20, if different from Report)		DDC DECLASSIFIED DEC 14 1977 E	
18. SUPPLEMENTARY NOTES 309 050			
19. KEY WORDS (Continue on reverse side if necessary and identify by block number) Clutter Detection Radar			
20. ABSTRACT (Continue on reverse side if necessary and identify by block number) We have calculated the probability of detecting either a Swerling-1 or Swerling-2 target immersed in both Rayleigh noise and log-normally distributed clutter. Results are presented which indicate the effect on detection of the number of pulses integrated, signal-to-noise ratio and the noise-to-clutter ratio.			

DD FORM 1 JAN 75 1473

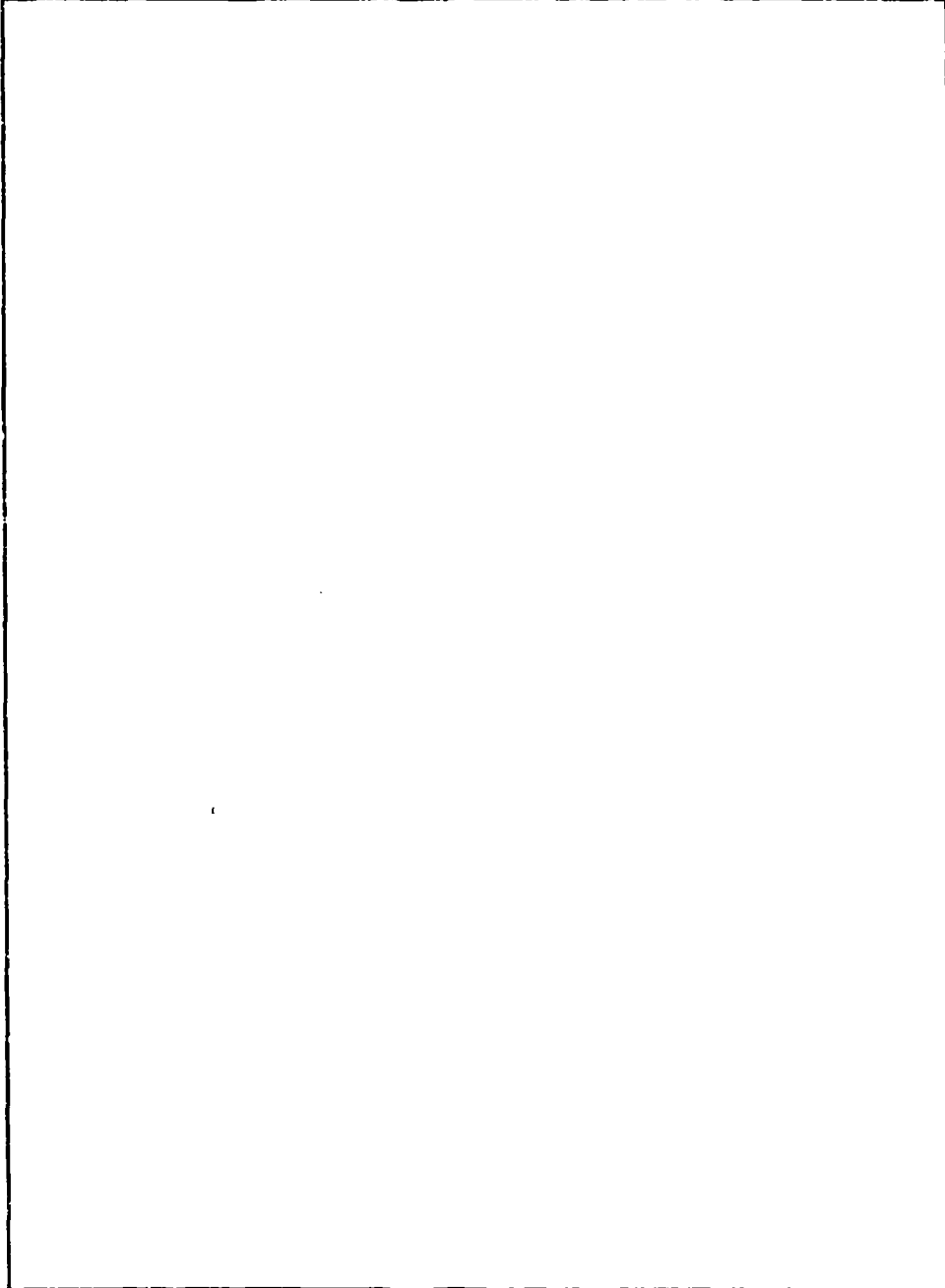
EDITION OF 1 NOV 65 IS OBSOLETE

Unclassified

SECURITY CLASSIFICATION OF THIS PAGE (When Data Entered)

*See*

SECURITY CLASSIFICATION OF THIS PAGE(When Data Entered)



SECURITY CLASSIFICATION OF THIS PAGE(When Data Entered)

## Preface

The author is grateful to Dr. Peter Wintersteiner of ARCON Corp. who programmed the integrals in Equations (35)-(37).

ACCESSION NO.	
YES	File Section <input checked="" type="checkbox"/>
NO	File Section <input type="checkbox"/>
YES	File Section <input type="checkbox"/>
NO	File Section <input type="checkbox"/>
DISTRIBUTION/AVAILABILITY CODES	
YES	SPECIAL <input type="checkbox"/>
NO	SPECIAL <input type="checkbox"/>
A	

## Contents

1. INTRODUCTION	9
2. THEORETICAL ANALYSIS	10
2.1 Target and Clutter Constant From Pulse-to-Pulse but Varying From Scan-to-Scan (Swerling 1)	10
2.2 Clutter Varying From Scan-to-Scan but Target Varying From Pulse-to-Pulse (Swerling-2 Target)	15
3. PROBABILITY OF FALSE ALARM AND DETECTION	18
4. NUMERICAL RESULTS	20
4.1 False-Alarm Probability	20
4.2 Probability of Detection for Swerling-2 Targets	23
4.3 Probability of Detection for Swerling-1 Targets	28
5. DISCUSSION	32
REFERENCES	33
APPENDIX A. Probability Density for a Constant Target	35
APPENDIX B. Derivation of Equation (38)	37
APPENDIX C. Derivation of Equation (40)	39

PREVIOUS PAGE NOT FILLED  
BLANK

## Illustrations

1. False-Alarm Probability for $N = 1$ , $\sigma = 0.7$	21
2. False-Alarm Probability for $N = 3$ , $\sigma = 0.7$	21
3. False-Alarm Probability for $N = 6$ , $\sigma = 0.7$	21
4. False-Alarm Probability for $N = 10$ , $\sigma = 0.7$	21
5. Effect of $\sigma$ on $P_f$ for $\beta = 3.16$ , $N = 1$	22
6. Effect of $\sigma$ on $P_f$ for $\beta = 3.16$ , $N = 10$	22
7. Probability of Detection (Swerling 2) for $P_f = 10^{-4}$ , $\beta = 0.316$ , $\sigma = 0.7$	23
8. Probability of Detection (Swerling 2) for $P_f = 10^{-4}$ , $\beta = 1.0$ , $\sigma = 0.7$	23
9. Probability of Detection (Swerling 2) for $P_f = 10^{-4}$ , $\beta = 3.16$ , $\sigma = 0.7$	23
10. Probability of Detection (Swerling 2) for $P_f = 10^{-4}$ , $\beta = 10$ , $\sigma = 0.7$	23
11. Probability of Detection (Swerling 2) for $P_f = 10^{-4}$ , $\beta = 100$ , $\sigma = 0.7$	25
12. Probability of Detection (Swerling 2) for $P_f = 10^{-6}$ , $\beta = 0.316$ , $\sigma = 0.7$	25
13. Probability of Detection (Swerling 2) for $P_f = 10^{-6}$ , $\beta = 1$ , $\sigma = 0.7$	25
14. Probability of Detection (Swerling 2) for $P_f = 10^{-6}$ , $\beta = 3.16$ , $\sigma = 0.7$	25
15. Probability of Detection (Swerling 2) for $P_f = 10^{-6}$ , $\beta = 10$ , $\sigma = 0.7$	26
16. Probability of Detection (Swerling 2) for $P_f = 10^{-6}$ , $\beta = 100$ , $\sigma = 0.7$	26
17. Effect of $\sigma$ on $P_{d2}$ for $P_f = 10^{-4}$ , $\beta = 3.16$	26
18. Effect of $\sigma$ on $P_{d2}$ for $P_f = 10^{-6}$ , $\beta = 3.16$	26
19. Probability of Detection (Swerling 1) for $P_f = 10^{-4}$ , $\beta = 0.316$ , $\sigma = 0.7$	29
20. Probability of Detection (Swerling 1) for $P_f = 10^{-4}$ , $\beta = 1$ , $\sigma = 0.7$	29
21. Probability of Detection (Swerling 1) for $P_f = 10^{-4}$ , $\beta = 3.16$ , $\sigma = 0.7$	29
22. Probability of Detection (Swerling 1) for $P_f = 10^{-4}$ , $\beta = 10$ , $\sigma = 0.7$	29
23. Probability of Detection (Swerling 1) for $P_f = 10^{-4}$ , $\beta = 100$ , $\sigma = 0.7$	30
24. Probability of Detection (Swerling 1) for $P_f = 10^{-6}$ , $\beta = 0.316$ , $\sigma = 0.7$	30
25. Probability of Detection (Swerling 1) for $P_f = 10^{-6}$ , $\beta = 1$ , $\sigma = 0.7$	30

## Illustrations

26. Probability of Detection (Swerling 1) for $P_f = 10^{-6}$ , $\beta = 3.16$ , $\sigma = 0.7$	30
27. Probability of Detection (Swerling 1) for $P_f = 10^{-6}$ , $\beta = 10$ , $\sigma = 0.7$	31
28. Probability of Detection (Swerling 1) for $P_f = 10^{-6}$ , $\beta = 100$ , $\sigma = 0.7$	31

## Tables

1. Comparison of $P_f$ as Calculated From Equation (38) With the Exact Result	22
2. Value of Signal-to-Noise Ratio $\alpha$ Required for $P_{d2} = 0.9, 0.99$ and $0.999$ When $P_f = 10^{-6}$ and $\sigma = 0.7$	27
3. Comparison of $P_{d2}$ Calculated From Equation (40) With the Exact Result for $\sigma = 0.7$ and $P_f = 10^{-6}$	28



## Detection of Targets in Noise and Clutter

### 1. INTRODUCTION

The probability density function (after detection and video integration) for a fluctuating target in gaussian noise has been known for some years now.<sup>1</sup> Similarly, results have also been obtained for the case of a fluctuating target immersed in log-normally distributed clutter.<sup>2,3</sup> However, it does not appear that any results have been obtained for the case of a fluctuating target immersed in both noise and clutter. Therefore, in this paper we will calculate the (post square-law detection) probability density function for the sum of  $N$  pulses, after video integration, for the case of a target immersed simultaneously in gaussian noise and log-normally distributed clutter. We shall consider principally the case when the clutter power is of the same order of magnitude as the noise power, because when the clutter power is very much larger than the noise power the results in<sup>2</sup> are appropriate, whereas when the noise power greatly exceeds the clutter power the results in<sup>1</sup> are adequate.

(Received for publication 21 July 1977)

1. Marcum, J., and Swerling, P. (1960) Studies of target detection by pulsed radar, IRE Trans. on Inform Theory IT-6:2.
2. Trunk, G., and George, S. (1970) Detection of targets in non-gaussian sea clutter, IEEE Trans. on Aerospace and Electronic Systems AES-6:620.
3. Schleher, D. (1975) Radar detection in log-normal clutter, IEEE International Radar Conference, IEEE Press (Publication No. 75 CH0938-1 AES), New York.

We shall present detailed numerical results for the probability of a false alarm and the probability of detection for both Swerling-1 and Swerling-2 targets.

## 2. THEORETICAL ANALYSIS

### 2.1 Target and Clutter Constant From Pulse-to-Pulse but Varying From Scan-to-Scan (Swerling 1)

Let us suppose we have a target immersed in gaussian noise and log-normally distributed clutter, and this target is to be detected using an N-pulse radar burst. If we assume that both the target and the clutter are constant from pulse-to-pulse but vary from scan-to-scan, then the single pulse return  $Re^{i\theta}$  can be written as

$$Re^{i\theta} = \rho + re^{i\phi} \quad , \quad (1)$$

where  $\rho$  represents the target-plus-clutter and  $r \exp(i\phi)$  is a complex phasor representing the noise, which is assumed to vary from pulse-to-pulse, and have the probability density (for  $r \geq 0$ )

$$p_n(r, \phi) = \frac{r}{2\pi\sigma_n^2} \exp\left(-\frac{r^2}{2\sigma_n^2}\right) \quad . \quad (2)$$

For mathematical convenience, we assume that the signal is to be detected using a square-law device. We are therefore interested in the probability distribution of the square,  $R^2$ , of the envelope of the received signal. If we define

$$x = \frac{\rho^2}{2\sigma_n^2} \quad ,$$

$$y = \frac{R^2}{2\sigma_n^2} \quad ,$$

and temporarily treat  $\rho$  as though it were a constant, because it does not vary from pulse-to-pulse, it is readily shown<sup>4</sup> that the conditional probability  $p(y|x)$  is

4. Beckmann, P. (1967) Probability in Communication Engineering, Harcourt, Brace and World, New York.

$$\begin{aligned}
 p(y|x) &= \exp(-x - y) I_0(2\sqrt{xy}) \quad \text{for } y \geq 0 \\
 &= 0 \quad \text{for } y < 0,
 \end{aligned} \tag{3}$$

where  $I_0(\dots)$  is the modified Bessel function. The characteristic function  $C_1(s|x)$  associated with  $p(y|x)$  is

$$\begin{aligned}
 C_1(s|x) &\equiv \int_0^\infty dy e^{-sy} p(y|x) \\
 &= e^{-x} \int_0^\infty dy e^{-(s+1)y} I_0(2\sqrt{xy}) \\
 &= (s+1)^{-1} \exp\left(-x + \frac{x}{s+1}\right).
 \end{aligned} \tag{4}$$

For N-pulse detection, we detect the sum of N different values  $y_n$  of the signal plus noise variables. That is,

$$Y = y_1 + y_2 + y_3 + \dots + y_N. \tag{5}$$

If the noise samples are statistically independent, then the characteristic function of the sum of the N samples is the product of their individual characteristic functions. Therefore, the characteristic function  $C_N(s|x)$  associated with Y is

$$C_N(s|x) = (s+1)^{-N} \exp\left(-Nx + \frac{Nx}{s+1}\right) \tag{6}$$

Now because the target and clutter fluctuate from scan-to-scan, we must therefore average (6) over the variable  $x = \rho^2/2\sigma_n^2$ . That is

$$\begin{aligned}
 C_N(s) &= \int_{-\infty}^{\infty} dx p(x) C_N(s|x) \\
 &= \int_{-\infty}^{\infty} \frac{dx p(x) \exp\left(-Nx + \frac{Nx}{s+1}\right)}{(s+1)^N}.
 \end{aligned} \tag{7}$$

where  $p(x)$  is the probability density of the random variable  $x$ . We shall calculate this later. Once  $C_N(c)$  is known, the probability density of  $Y = y_1 + y_2 + \dots + y_N$  is

$$\begin{aligned} P_N(Y) &= \frac{1}{2\pi i} \int_{\Delta-i\infty}^{\Delta+i\infty} ds C_N(s) e^{sY} \\ &= \int_{-\infty}^{\infty} dx p(x) e^{-Nx} G_N(x, Y) \quad , \end{aligned} \quad (8)$$

where

$$G_N(x, Y) = \frac{1}{N^{N-1}} \left( \frac{d}{dx} \right)^{N-1} I_0(2\sqrt{NxY}) = \left( \frac{Y}{Nx} \right)^{(N-1)/2} I_{N-1}(2\sqrt{NxY}) \quad . \quad (9)$$

The result in Eq. (9) follows from the  $(N - 1)$  fold differentiation of both sides of the known result

$$\frac{1}{2\pi i} \int_{\Delta-i\infty}^{\Delta+i\infty} ds \frac{\exp(sY + \frac{Nx}{s+1})}{(s+1)} = e^{-Y} I_0(2\sqrt{NxY}) \quad . \quad (10)$$

In order to evaluate Eq. (8) for  $p(y)$ , we must first obtain  $p(x)$ . We recall that  $\rho$  is the sum of the target and clutter and can be written as

$$\rho = \mu \exp(i\lambda) + \eta \exp(i\psi) \quad (11)$$

where  $\mu \exp(i\lambda)$  is a phasor representing the target return and  $\eta \exp(i\psi)$  is a phasor representing the clutter signal. For a Rayleigh target, we know that

$$\begin{aligned} p_t(\mu, \lambda) &= \frac{\mu}{2\pi\sigma_t^2} \exp\left(-\frac{\mu^2}{2\sigma_t^2}\right) \quad \text{for } \mu \geq 0 \\ &= 0 \quad \text{for } \mu < 0 \quad , \end{aligned} \quad (12)$$

and the log-normal clutter is governed by the probability density

$$p_c(\eta, \psi) = (2\pi)^{-3/2} (\sigma\eta)^{-1} \exp \left[ -\frac{\left( \ln \frac{\eta}{\eta_0} \right)^2}{2\sigma^2} \right] \quad \text{for } \eta \geq 0 \quad (13)$$

$$= 0 \quad \text{for } \eta < 0$$

The quantity  $\eta_0$  in (13) is the median value of  $\eta$ . Also, the standard deviation  $\sigma$  has been estimated<sup>2,3</sup> to be 0.7 for low-sea-state clutter, 1.1 for ground clutter, and as high as 1.6 for high-sea-state clutter.

The probability density for the envelope of a Rayleigh plus log-normal phasor is given in Chapter 4 of Beckmann<sup>4</sup> and can be written as

$$p_{tc}(\rho) = \rho \exp \left( -\frac{\rho^2}{2\sigma_t^2} \right) \int_0^\infty d\tau F(\tau) I_0 \left( \frac{\rho\tau}{\sigma_t^2} \right) \quad \text{for } \rho \geq 0 \quad (14)$$

$$= 0 \quad \text{for } \rho < 0,$$

where

$$F(\tau) = (2\pi)^{-1/2} (\sigma\sigma_t^2\tau)^{-1} \exp \left[ -\frac{\tau^2}{2\sigma_t^2} - \frac{\ln^2 \left( \frac{\tau}{\eta_0} \right)}{2\sigma^2} \right].$$

If we recall that  $x = \rho^2/2\sigma_n^2$ , it is easy to show that

$$p_{tc}(x) = \sigma_n^2 e^{-bx} \int_0^\infty d\tau F(\tau) I_0 \left[ (2x)^{1/2} \frac{\sigma_n\tau}{\sigma_t^2} \right] \quad \text{for } x \geq 0 \quad (15)$$

where

$$b = (\sigma_n/\sigma_t)^2.$$

We now use (15) in (8) and set  $\eta = \tau/\sigma_t$  and  $\psi = \tau/\sigma_t^2$ . After some manipulation, we obtain

$$p_N(y) = \gamma e^{-Y} Y^{(N-1)/2} \int_0^\infty \frac{d\xi I_{N-1}(2\sqrt{Y\xi}) e^{-(1+\gamma)\xi} M(\xi)}{(\xi)^{(N-1)/2}} \quad \text{for } Y \geq 0$$

$$= 0 \quad \text{for } Y < 0$$
(16)

where

$$M(\xi) = \frac{1}{(2\pi)^{1/2}\sigma} \int_0^\infty \frac{d\eta}{\eta} I_0[\eta(2\gamma\xi)^{1/2}] \exp\left\{-\frac{\eta^2}{2} - \frac{\eta^2(\alpha\beta\eta^2)}{8\sigma^2}\right\}$$
(17)

$$\gamma = \frac{1}{N\alpha}$$
(18)

$$\beta = \left(\frac{\sigma_n}{\eta_0}\right)^2 = \text{noise to clutter ratio}$$
(19)

$$\alpha = \left(\frac{\sigma_t}{\sigma_n}\right)^2 = \text{signal to noise ratio}$$
(20)

Equation (16) is the probability density for the sum of  $N$  pulses (following square-law detection) received from a slowly varying target immersed in slowly varying clutter but rapidly varying noise. This can be thought of as a Swerling-1 target immersed in Rayleigh noise and Swerling-1 clutter.

As a check on the validity of (16), we can study the limit as the clutter power vanishes ( $\beta \rightarrow \infty$ ). In this case, (17) should reduce to the usual Swerling-1 result. When  $\beta \rightarrow \infty$ , it is clear that the only contribution to the integration over  $\eta$  in (17) comes from  $\eta$  very near zero. Therefore, we can expand the integrand in a Taylor series about  $\eta = 0$ . This gives

$$M(\xi) \xrightarrow{\beta \rightarrow \infty} \frac{1}{(2\pi)^{1/2}\sigma} \int_0^\infty \frac{d\eta}{\eta} \exp\left[-\frac{\eta^2(\alpha\beta\eta^2)}{8\sigma^2}\right] = 1$$

If we set  $M(\xi) = 1$  in (16) we readily find using p. 187 of Bateman<sup>5</sup> that for  $Y \geq 0$

$$p_N(Y) \xrightarrow{\beta \rightarrow \infty} \frac{\left(\frac{1}{N\alpha}\right) \left(1 + \frac{1}{N\alpha}\right)^{N-2} \exp\left(-\frac{Y}{1 + N\alpha}\right) \gamma\left(N-1, \frac{Y}{1 + \frac{1}{N\alpha}}\right)}{(N-2)!} \quad (21)$$

where  $\gamma(N, x)$  is the incomplete gamma function defined on p. 387 of Bateman.<sup>5</sup> Equation (21) is precisely the well-known result for a Swerling-1 target in Rayleigh noise, as is seen by comparison with the results in Section 3.5 of Berkowitz.<sup>6</sup>

An additional check is obtained by studying the result for  $N = 1$ . For  $y \geq 0$ , (16) becomes in this case

$$p_1(Y) = \frac{\gamma \exp\left[-\frac{\gamma Y}{1 + \gamma}\right]}{(2\pi)^{1/2} \sigma(1 + \gamma)} \int_0^\infty \frac{d\eta}{\eta} I_0\left[\frac{\eta(2\gamma Y)^{1/2}}{1 + \gamma}\right] \exp\left\{-\frac{\eta^2}{2(1 + \gamma)} - \frac{i n^2(\alpha\beta\eta^2)}{8\sigma^2}\right\} \quad (22)$$

which is the well-known result for the sum of two Rayleigh and one log-normal random variables. Equation (22) is also appropriate for the N-pulse case in the limit when the noise samples are completely correlated from pulse-to-pulse, as opposed to the case we have considered here with the noise samples statistically independent from pulse-to-pulse.

## 2.2 Clutter Varying From Scan-to-Scan but Target Varying From Pulse-to-Pulse (Swerling-2 Target)

When the target varies so rapidly that its cross section changes from pulse-to-pulse (Swerling-2 Target) but the clutter is constant from pulse-to-pulse (where the clutter is assumed to vary from scan-to-scan) we can replace Eq. (1) by

$$R e^{i\theta} = u + v e^{i\delta} \quad (23)$$

where  $u$  represents the clutter and  $v \exp(i\delta)$  is a phasor representing the target plus noise. For a Rayleigh target immersed in Rayleigh noise (that is, the noise envelope is Rayleigh, although the quadrature components are gaussian), the joint probability density of  $v$  and  $\delta$  is given by (for  $v \geq 0$ )

5. Erdelyi, A., et al (1954) Tables of Integral Transform (Bateman Manuscript Project), McGraw-Hill, New York.

6. Berkowitz, R. (1965) Modern Radar, Wiley, New York.

$$p_{tn}(v, \delta) = \frac{v}{2\pi(\sigma_n^2 + \sigma_t^2)} \exp \left\{ -\frac{v^2}{2(\sigma_n^2 + \sigma_t^2)} \right\} \quad (24)$$

where  $\sigma_n^2$  is the noise variance and  $\sigma_t^2$  is the target variance. We are again interested in obtaining the probability density of the square of the envelope of the total received signal. Let us define

$$z = \frac{u^2}{2(\sigma_n^2 + \sigma_t^2)}$$

$$y' = \frac{R^2}{2(\sigma_n^2 + \sigma_t^2)} = \frac{y}{1 + \alpha}$$

where  $y$  is the same variable defined following Eq. (2) and  $\alpha$  is defined in (20). If we temporarily treat  $u$  as a constant because it does not vary from pulse-to-pulse (but only from scan-to-scan), it is straightforward to show<sup>4</sup> that

$$\begin{aligned} p(y'|z) &= \exp(-z - y') I_0[2(z y')^{1/2}] \quad \text{for } y' \geq 0 \\ &= 0 \quad \text{for } y' < 0 \end{aligned} \quad (25)$$

which gives a single-pulse characteristic function

$$C_1(s|z) = (s + 1)^{-1} \exp \left( -z + \frac{z}{s + 1} \right) \quad (26)$$

For  $N$ -pulse detection, we detect the sum of  $N$  different values  $y'_n$ . In particular

$$Y' = y'_1 + y'_2 + \dots + y'_N \quad (27)$$

If we assume that the target plus noise variables are statistically independent from pulse-to-pulse, the  $N$ -pulse characteristic function is the product of the single pulse ones and we get



$$C_N(s|z) = (s+1)^{-N} \exp \left[ -Nz + \frac{Nz}{s+1} \right] \quad (28)$$

Because the clutter varies from scan-to-scan, we must next average (28) over the clutter probability density. This gives

$$C_N(s) = \int_{-\infty}^{\infty} \frac{dz p_c(z) \exp \left( -Nz + \frac{Nz}{s+1} \right)}{(s+1)^N} \quad (29)$$

where  $p_c(z)$  is the probability density of the square of the clutter envelope. If we write the clutter  $u$  as the random phasor  $u = \eta \exp(i\psi)$ , it is evident that  $p_c(\eta, \psi)$  is given by (13). In terms of the variable  $z = u^2/2(\sigma_n^2 + \sigma_t^2)$ , this becomes

$$p_c(z) = \left[ 2(2\pi)^{1/2} \sigma z \right]^{-1} \exp \left[ -\frac{\ln^2(2hz)}{8\sigma^2} \right] \quad \text{for } z \geq 0$$

$$= 0 \quad \text{for } z < 0 \quad (30)$$

where  $h = (\sigma_n^2 + \sigma_t^2)/\eta_0^2$ . If we use (30) in (29), we get

$$C_N(s) = \frac{1}{2(2\pi)^{1/2} \sigma (s+1)^N} \int_0^{\infty} \frac{dz}{z} \exp \left[ -Nz + \frac{Nz}{s+1} - \frac{\ln^2(2hz)}{8\sigma^2} \right] \quad (31)$$

so that

$$p_N(Y) = \frac{1}{2\pi i} \int_{\Delta-i\infty}^{\Delta+i\infty} ds e^{sY'} C_N(s)$$

is given by

$$p_N(Y') = \frac{e^{-Y'}}{2(2\pi)^{1/2} \sigma} \int_0^{\infty} \frac{dz}{z} \exp \left[ -Nz - \frac{\ln^2(2hz)}{8\sigma^2} \right] G_N(z, Y') \quad \text{for } Y' \geq 0$$

$$= 0 \quad \text{for } Y' < 0 \quad (32)$$

where  $G_N(z, Y')$  is given by (9). Finally, if we let  $\xi = Nz$  we can rewrite (32) as

$$p_N(Y') = \frac{(Y')^{(N-1)/2} e^{-Y'}}{2(2\pi)^{1/2} \sigma} \int_0^\infty \frac{d\xi}{(\xi)^{(N+1)/2}} I_{N-1} \left[ 2(Y'\xi)^{1/2} \right] \exp \left[ -\xi - \frac{\ln^2 \left( \frac{2h\xi}{N} \right)}{8\sigma^2} \right]$$

for  $Y' \geq 0$  (33)

$$= 0 \quad \text{for } Y' < 0$$

As a check on the validity of (33), we can consider the limiting case when the clutter is absent ( $h \rightarrow \infty$ ). In this case, it is evident that the dominant contribution to the  $\xi$  integral comes from  $\xi$  near zero. Therefore, we may expand the integrand in a Taylor series about  $\xi = 0$ . If this is done, the  $\xi$  integral may be performed and we find (for  $Y' \geq 0$ )

$$p_N(Y') = \frac{(Y')^{N-1} e^{-Y'}}{(N-1)!}$$

which is identical with the well-known<sup>6</sup> result for the N-pulse sum for a Swerling-2 target in Rayleigh noise.

### 3. PROBABILITY OF FALSE ALARM AND DETECTION

The probability of a false alarm is the probability that the received signal exceeds some threshold level  $Y_0$  when there is no target present. In the limit when the target is absent, it is readily demonstrated that for  $Y \geq 0$ , (16) becomes

$$p_N(Y) = \frac{(Y)^{(N-1)/2} e^{-Y}}{2(2\pi)^{1/2} \sigma} \int_0^\infty \frac{d\xi}{(\xi)^{(N+1)/2}} I_{N-1} \left[ 2(Y\xi)^{1/2} \right] \exp \left[ -\xi - \frac{\ln^2 \left( \frac{2\beta\xi}{N} \right)}{8\sigma^2} \right]$$

(34)

Therefore, the probability of a false alarm for an N-pulse detection system is

$$P_f = \frac{1}{2(2\pi)^{1/2}\sigma} \int_{Y_0}^{\infty} dY e^{-Y} (Y)^{(N-1)/2} \int_0^{\infty} \frac{d\xi I_{N-1} \left[ 2(Y\xi)^{1/2} \right] \exp \left[ -\xi - \frac{\ln^2 \left( \frac{2\beta\xi}{N} \right)}{8\sigma^2} \right]}{(\xi)^{(N+1)/2}} d\xi \quad (35)$$

The probability of detecting a Swerling-1 Target in noise and slowly varying clutter can be obtained from (16) and is the probability that  $Y \geq Y_0$  when a target is present. This is

$$P_{d1} = \gamma \int_{Y_0}^{\infty} dY e^{-Y} (Y)^{(N-1)/2} \int_0^{\infty} \frac{d\xi I_{N-1} \left[ 2(Y\xi)^{1/2} \right] M(\xi) e^{-(1+\gamma)\xi}}{(\xi)^{(N+1)/2}} d\xi \quad (36)$$

Also, the probability of detecting a Swerling-2 target in noise plus slowly varying clutter is the probability that  $Y' \geq Y_0/(1+\alpha)$  because  $Y' = Y/(1+\alpha)$ . Therefore, from (33) we have

$$P_{d2} = \frac{1}{2(2\pi)^{1/2}\sigma} \int_{\frac{Y_0}{1+\alpha}}^{\infty} dY e^{-Y} (Y)^{(N-1)/2} \int_0^{\infty} \frac{d\xi I_{N-1} \left[ 2(Y\xi)^{1/2} \right] \exp \left[ -\xi - \frac{\ln^2 (2h\xi N^{-1})}{8\sigma^2} \right]}{(\xi)^{(N+1)/2}} d\xi \quad (37)$$

It is easy to demonstrate, that  $P_{d1} = P_{d2}$  for  $N = 1$ .

In the next section, we will present numerical results for  $P_f$ ,  $P_{d1}$  and  $P_{d2}$ .

#### 4. NUMERICAL RESULTS

Before presenting our results it is useful to reemphasize once again our definitions for signal-to-noise and noise-to-clutter ratios, since they may differ somewhat from those used by other authors. They are

$$\alpha \equiv \frac{\sigma_t^2}{\sigma_n^2} = \text{signal-to-noise ratio,}$$

$$\beta \equiv \frac{\sigma_n^2}{\eta_c^2} = \text{noise to median-clutter ratio,}$$

$N$  = number of independent pulses integrated,

$P_f$  = probability of a false alarm,

$P_{d1}$  = probability of detecting a Swerling-1 target in noise varying from pulse-to-pulse and clutter varying from scan-to-scan,

$P_{d2}$  = probability of detecting a Swerling-2 target in noise varying from pulse-to-pulse and clutter varying from scan-to-scan.

##### 4.1 False-Alarm Probability

By using (35), we have calculated the probability  $P_f$  of a false alarm as a function of the threshold  $Y_o = R_o^2/2\sigma_n^2$ , for a number of different values of the noise-to-clutter ratio  $\beta$ . These results, with the standard deviation  $\sigma$  of the log normal distribution set equal to 0.7, are presented in Figures 1-4. We observe that the probability of a false alarm is significantly affected by the value of  $\beta$ . It is even more strongly affected by the value of  $\sigma$  as can be seen from the results in Figures 5 and 6.

From the nature of the curves in Figures 1-6 it is clear that for large values of  $Y_o$  (that is, small false alarm probabilities),  $P_f$  is a function of  $\beta Y_o/N$ . It is demonstrated in Appendix B that for  $Y_o$  large, we may approximate (35) by

$$P_f \approx \frac{1}{2} \operatorname{erfc} \left[ \frac{1}{2^{3/2} \sigma} \ln \left( \frac{2 \beta Y_o}{N} \right) \right] \quad (38)$$

where  $\operatorname{erfc}$  is the complementary error function defined by

$$\operatorname{erfc}(z) = \frac{2}{(\pi)^{1/2}} \int_z^\infty e^{-t^2} dt \approx \frac{1}{(\pi)^{1/2} z} \exp(-z^2) \quad (39)$$

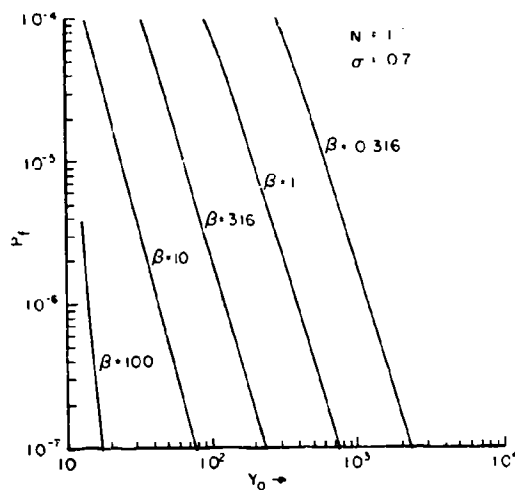


Figure 1. False-Alarm Probability for  $N = 1$ ,  $\sigma = 0.7$

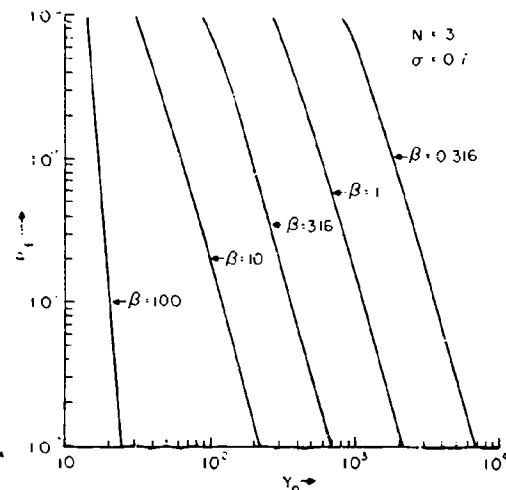


Figure 2. False-Alarm Probability for  $N = 3$ ,  $\sigma = 0.7$

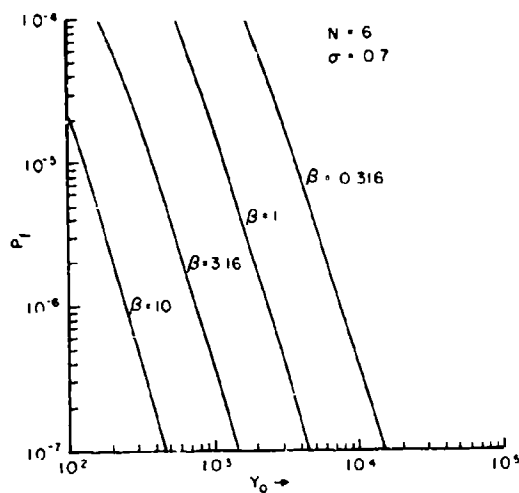


Figure 3. False-Alarm Probability for  $N = 6$ ,  $\sigma = 0.7$

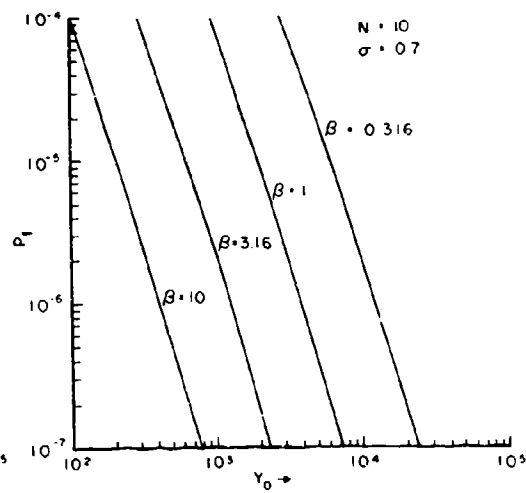


Figure 4. False-Alarm Probability for  $N = 10$ ,  $\sigma = 0.7$

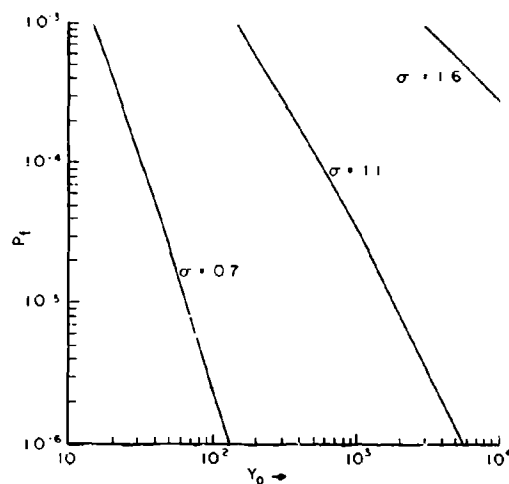


Figure 5. Effect of  $\sigma$  on  $P_f$  for  $\beta = 3.16$ ,  $N = 1$

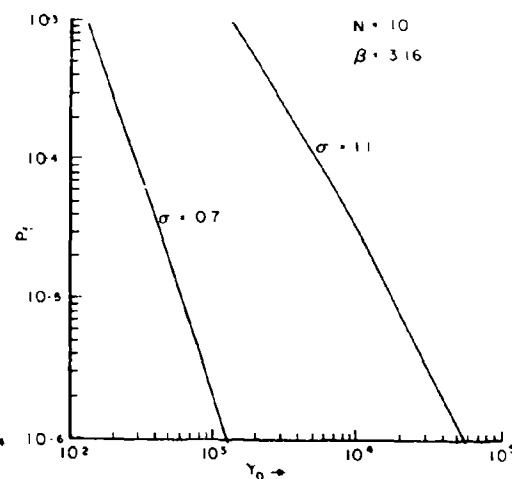


Figure 6. Effect of  $\sigma$  on  $P_f$  for  $\beta = 3.16$ ,  $N = 10$

Table 1. Comparison of  $P_f$  as Calculated From Equation (38) With the Exact Result

$\sigma$	$N$	$\beta$	$Y_0$	$P_f$ (exact)	$P_f$ (calculated from Equation (38))
0.7	1	1	300	$2.55 \times 10^{-6}$	$2.57 \times 10^{-6}$
0.7	1	1	500	$4.20 \times 10^{-7}$	$4.20 \times 10^{-7}$
0.7	3	1	1000	$1.75 \times 10^{-6}$	$1.79 \times 10^{-6}$
0.7	10	1	5000	$4.10 \times 10^{-7}$	$4.20 \times 10^{-7}$
1.1	1	10	4000	$2.0 \times 10^{-7}$	$2.12 \times 10^{-7}$

The final approximation in (39) is valid for  $z$  large, which is usually the case of interest. A comparison in Table 1 of numerical results calculated from (38) with the curves in Figures 1-6 indicates that (38) is an excellent approximation to (35) as long as  $Y_0$  is large (that is,  $P_f$  small). Therefore, because in most practical problems we require a small value for  $P_f$ , Eq. (38) is a very useful approximation.

## 1.2 Probability of Detection for Swerling-2 Targets

We now present some numerical results for the probability of detecting a Swerling-2 target immersed in Rayleigh noise which varies from pulse-to-pulse and log-normally distributed clutter which fluctuates from scan-to-scan. By using Eq. (37), we have calculated the probability of detection  $P_{d2}$  for false-alarm probabilities of  $10^{-4}$  and  $10^{-6}$ . These calculations have been performed, assuming  $\sigma = 0.7$ , for a number of values of  $\beta$  and  $N$ , and are presented in Figures 7-16. For convenience we have also presented in Table 2 the values of the signal-to-noise ratio  $\alpha$  required for  $P_{d2} = 0.90, 0.99$  and  $0.999$ , for a number of different values of noise-to-clutter ratio  $\beta$  and pulses integrated.

The effect on  $P_{d2}$  of changing the standard deviation  $\sigma$  of the log-normal distribution is illustrated in Figures 17 and 18. We note that a change in  $\sigma$  from 0.7 to 1.1, results in more than one order of magnitude change in the value of signal to noise ratio  $\alpha$  required for a given probability of detection  $P_{d2}$ . For the case of vanishing clutter  $\beta \rightarrow \infty$ , our numerical data compares well with the data in reference 1 for a Swerling-2 target immersed in Rayleigh noise. In the opposite limit of vanishing noise  $\beta \rightarrow 0$  we can compare our results with those of Trunk<sup>7</sup> only for  $N = 1$ , because Trunk has considered the case when the clutter varies from pulse-to-pulse and we have considered the limit when the clutter varies only from scan-to-scan.

From Figures 7-18, we note that large signal-to-noise ratios are usually required for high detection probabilities. This suggests that it might be useful to have a large  $\alpha$  approximation to (37). For large  $\alpha$ , it is shown in Appendix C that (37) can be approximated as

$$P_{d2} \approx \exp \left( -\frac{Y_o}{1 + \alpha} \right) \sum_{m=0}^{N-1} \left( \frac{Y_o}{1 + \alpha} \right)^m \frac{1}{m!} \quad (40)$$

A comparison in Table 3 of numerical results calculated from (40) with the computed data in Figures 7-18 indicates that (40) is quite an excellent approximation for  $P_{d2}$  provided  $\alpha\beta/N \gg 1$ . This encompasses nearly the entire range of practical interest (that is,  $P_{d2} > 0.5$ ). Therefore, in quite a number of practical situations it is not necessary to numerically evaluate the integrals in (37), and Eq. (40) can be used.

7. Trunk, G. (1971) Further results on the detection of targets in non-gaussian sea clutter, IEEE Trans. on Aerospace and Electronic Systems AES-7:553.

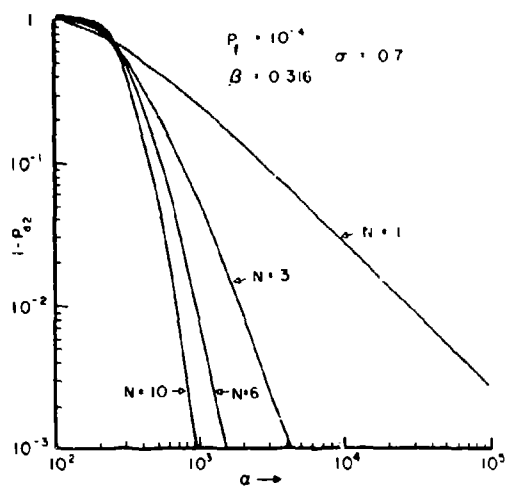


Figure 7. Probability of Detection (Swirling 2) for  $P_f = 10^{-4}$ ,  $\beta = 0.316$ ,  $\sigma = 0.7$

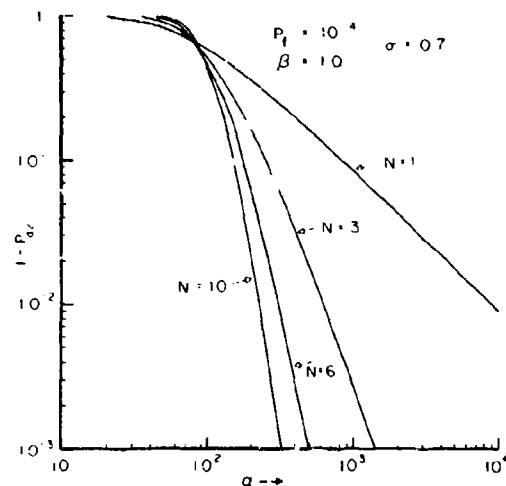


Figure 8. Probability of Detection (Swirling 2) for  $P_f = 10^{-4}$ ,  $\beta = 1.0$ ,  $\sigma = 0.7$

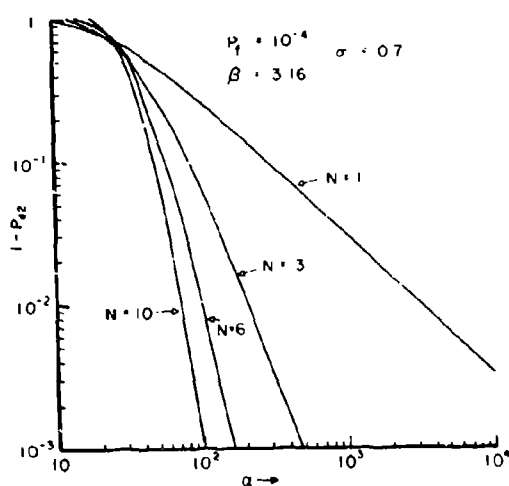


Figure 9. Probability of Detection (Swirling 2) for  $P_f = 10^{-4}$ ,  $\beta = 3.16$ ,  $\sigma = 0.7$

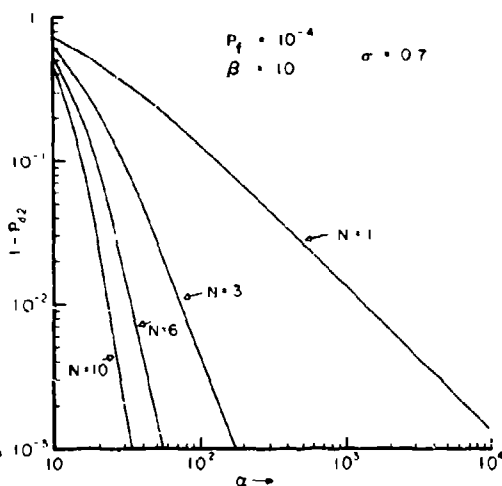


Figure 10. Probability of Detection (Swirling 2) for  $P_f = 10^{-4}$ ,  $\beta = 10$ ,  $\sigma = 0.7$



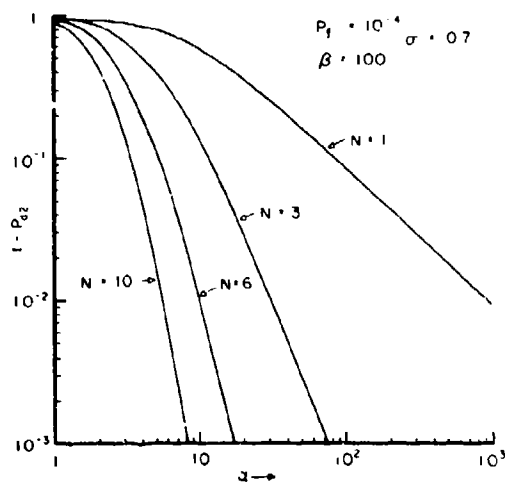


Figure 11. Probability of Detection (Swerling 2) for  $P_f = 10^{-4}$ ,  $\beta = 100$ ,  $\sigma = 0.7$

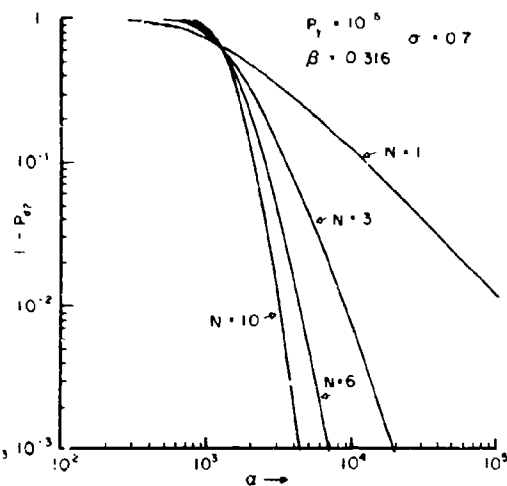


Figure 12. Probability of Detection (Swerling 2) for  $P_f = 10^{-6}$ ,  $\beta = 0.316$ ,  $\sigma = 0.7$

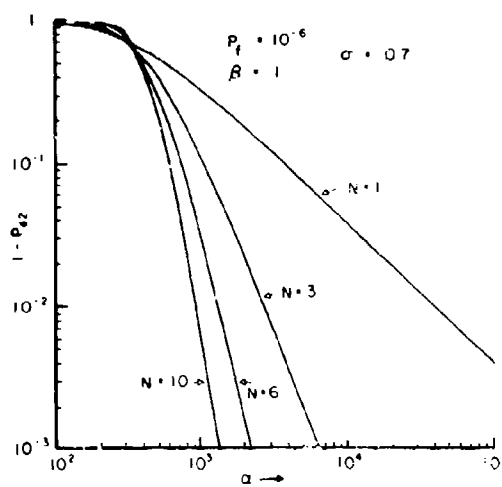


Figure 13. Probability of Detection (Swerling 2) for  $P_f = 10^{-6}$ ,  $\beta = 1$ ,  $\sigma = 0.7$

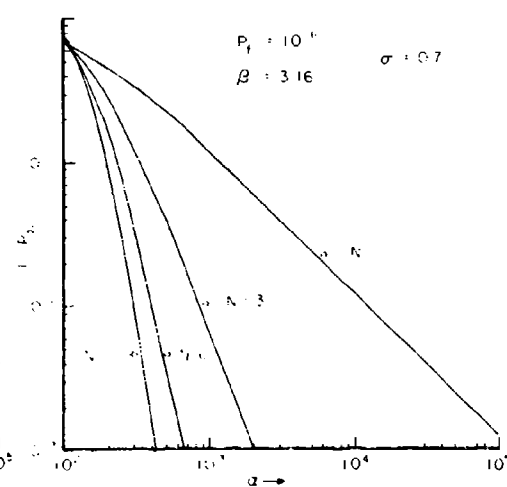


Figure 14. Probability of Detection (Swerling 2) for  $P_f = 10^{-6}$ ,  $\beta = 3.16$ ,  $\sigma = 0.7$

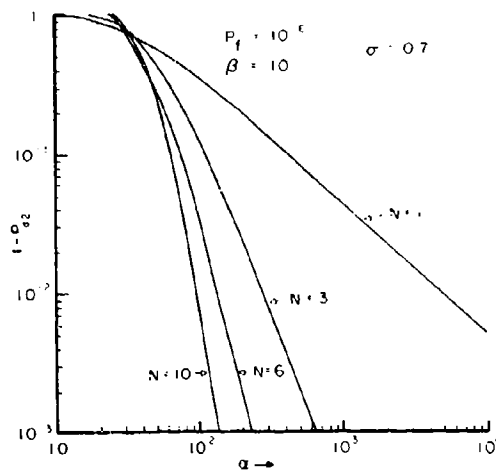


Figure 15. Probability of Detection (Swirling 2) for  $P_f = 10^{-6}$ ,  $\beta = 10$ ,  $\sigma = 0.7$

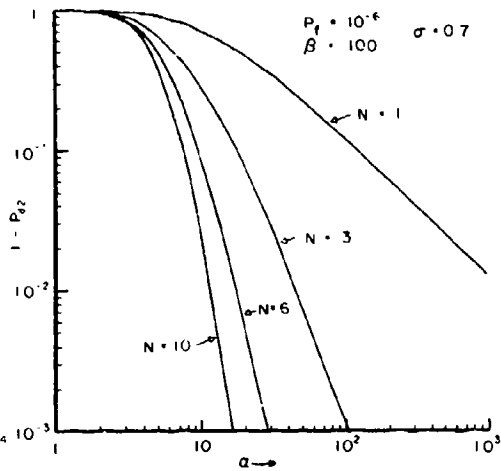


Figure 16. Probability of Detection (Swirling 2) for  $P_f = 10^{-6}$ ,  $\beta = 100$ ,  $\sigma = 0.7$

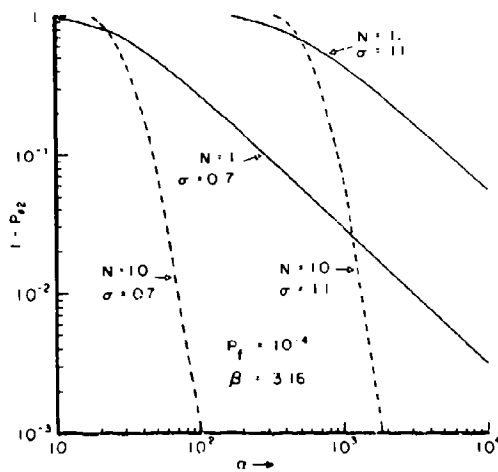


Figure 17. Effect of  $\sigma$  on  $P_{d2}$  for  $P_f = 10^{-4}$ ,  $\beta = 3.16$

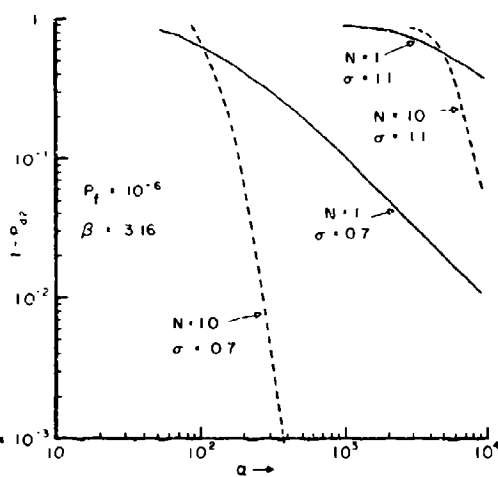


Figure 18. Effect of  $\sigma$  on  $P_{d2}$  for  $P_f = 10^{-6}$ ,  $\beta = 3.16$

Table 2. Value of Signal-to-Noise Ratio  $\alpha$  Required for  $P_{d2} = 0.9, 0.99$  and  $0.999$  When  $P_f = 10^{-6}$  and  $c = 0.7$

$\beta$	$P_{d2} = 0.9$	$P_{d2} = 0.99$	$P_{d2} = 0.999$
N = 1			
0.316	$1.177 \times 10^4$	$1.234 \times 10^5$	$1.239 \times 10^6$
1.0	$3.701 \times 10^3$	$3.880 \times 10^4$	$3.900 \times 10^5$
3.16	$1.185 \times 10^3$	$1.244 \times 10^4$	$1.244 \times 10^5$
10.0	$4.113 \times 10^2$	$4.321 \times 10^3$	$4.341 \times 10^4$
100.0	$1.329 \times 10^2$	$1.403 \times 10^3$	$1.410 \times 10^4$
N = 3			
0.316	3380	8500	$1.925 \times 10^4$
1.0	1055	2680	$6.100 \times 10^3$
3.16	348	855	$1.950 \times 10^3$
10.0	113	280	$6.40 \times 10^2$
100.0	17.7	46	$1.07 \times 10^2$
N = 6			
0.316	2350	4150	6650
1.0	640	1300	2120
3.16	234	412	660
10.0	75.5	135	240
100.0	9.7	17.8	29.5
N = 10			
0.316	1980	3000	4350
1.0	620	937	1300
3.16	197	298	415
10.0	64	96	137
100.0	7.6	12	17

Table 3. Comparison of  $P_{d2}$  Calculated From Equation (40) With the Exact Result for  $\sigma = 0.7$  and  $P_f = 10^{-6}$

$\beta$	$\alpha$	N	$Y_o$	$P_{d2}$ (exact)	$P_{d2}$ (calculated from Equation (40))
1	1000	1	390	0.67	0.68
1	1000	3	1170	0.89	0.89
1	1000	6	2350	0.968	0.967
1	1000	10	3900	0.994	0.9932
10	100	1	44	0.65	0.65
10	100	3	123	0.875	0.876
10	100	6	240	0.965	0.966
10	100	10	405	0.9922	0.9918

### 4.3 Probability of Detection for Swerling-1 Targets

We now calculate the probability of detecting a Swerling-1 target immersed in log-normal clutter which varies from scan-to-scan and Rayleigh noise which varies from pulse-to-pulse. By using (36), we have computed the probability of detection  $P_{d1}$  for false-alarm probabilities of  $10^{-4}$  and  $10^{-6}$ . These calculations for  $\sigma = 0.7$  and a number of different values of  $\beta$  and N are presented in Figures 19-28. From Figures 19-28, we observe that large signal-to-noise ratios  $\alpha$  are usually required for high probabilities of detection. For large  $\alpha$ , it is readily demonstrated\* that

$$P_{d1} \approx \left(1 + \frac{1}{N\alpha}\right)^{N-1} \exp \left\{ -\frac{Y_o}{1 + N\alpha} \right\} \quad (41)$$

A comparison of numerical results calculated from (41) with the computed data in Figures 19-28 indicates that (41) is an excellent approximation for  $P_{d1}$  whenever  $P_{d1} > 0.7$ .

\*The proof parallels that in Appendix C. In particular, observe that for large  $\alpha$  the integrand in (17) can be expanded in a Taylor series about  $\eta = 0$ . This gives  $M(\xi) = 1$ . Upon setting  $M(\xi) = 1$  in (36), we can readily do the  $\xi$  and  $y$  integrations.

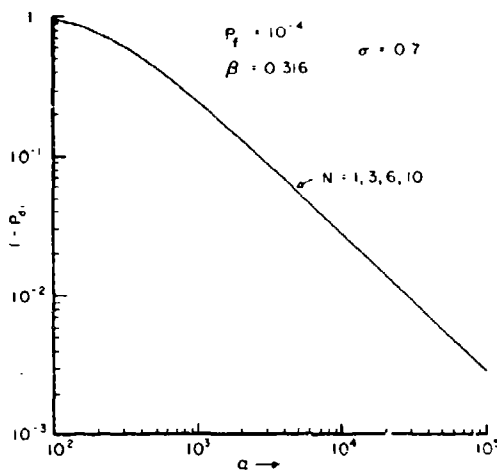


Figure 19. Probability of Detection (Swerling 1) for  $P_f = 10^{-4}$ ,  $\beta = 0.316$ ,  $\sigma = 0.7$

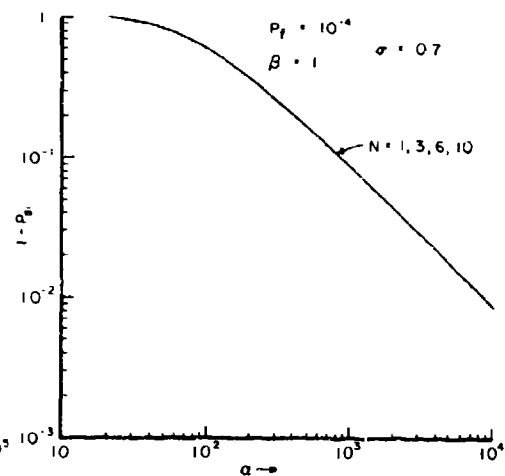


Figure 20. Probability of Detection (Swerling 1) for  $P_f = 10^{-4}$ ,  $\beta = 1$ ,  $\sigma = 0.7$

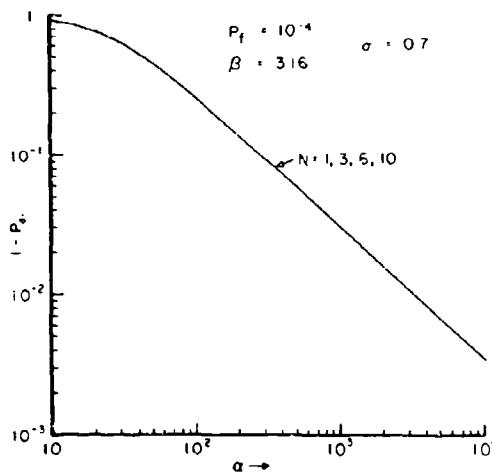


Figure 21. Probability of Detection (Swerling 1) for  $P_f = 10^{-4}$ ,  $\beta = 3.16$ ,  $\sigma = 0.7$

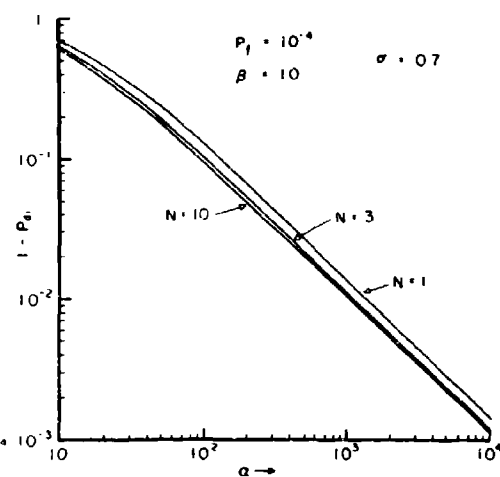


Figure 22. Probability of Detection (Swerling 1) for  $P_f = 10^{-4}$ ,  $\beta = 10$ ,  $\sigma = 0.7$

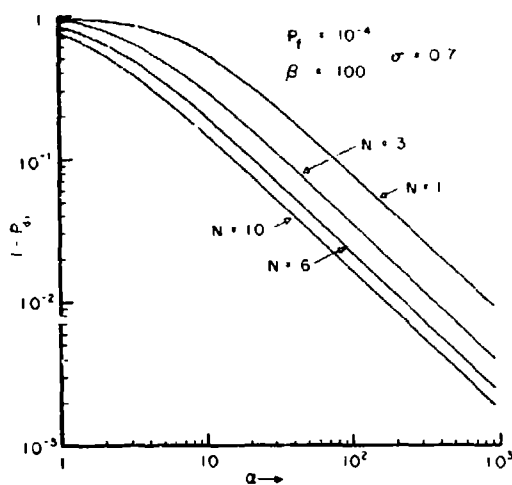


Figure 23. Probability of Detection (Swirling 1) for  $P_f = 10^{-4}$ ,  $\beta = 100$ ,  $\sigma = 0.7$

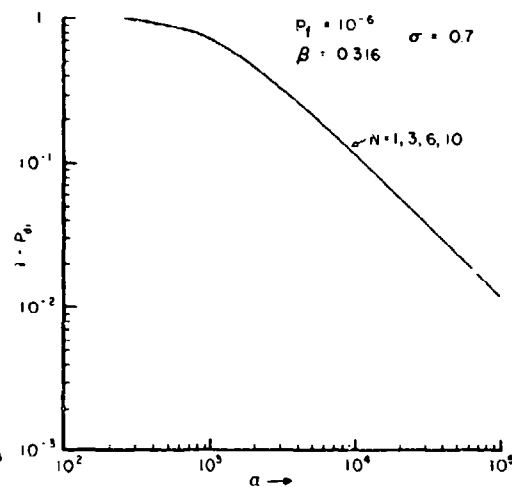


Figure 24. Probability of Detection (Swirling 1) for  $P_f = 10^{-6}$ ,  $\beta = 0.316$ ,  $\sigma = 0.7$

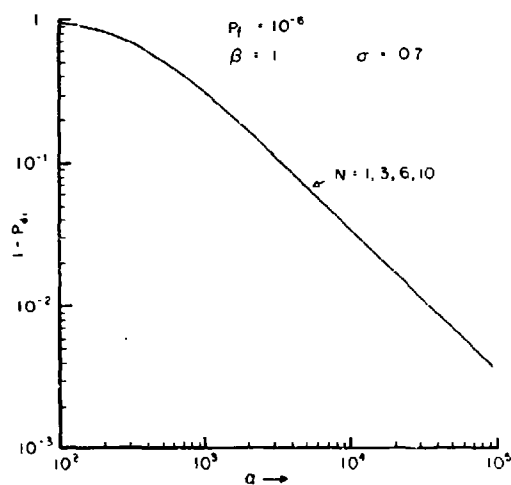


Figure 25. Probability of Detection (Swirling 1) for  $P_f = 10^{-6}$ ,  $\beta = 1$ ,  $\sigma = 0.7$

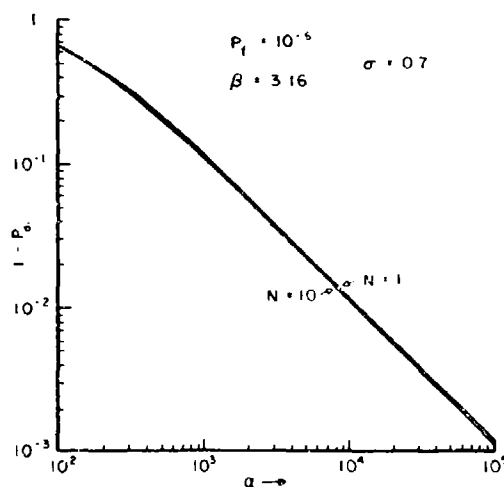


Figure 26. Probability of Detection (Swirling 1) for  $P_f = 10^{-6}$ ,  $\beta = 3.16$ ,  $\sigma = 0.7$

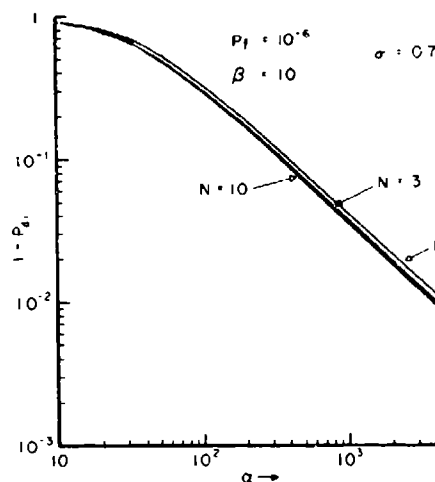


Figure 27. Probability of Detection (Swerling 1) for  $P_f = 10^{-6}$ ,  $\beta = 10$ ,  $\sigma = 0.7$

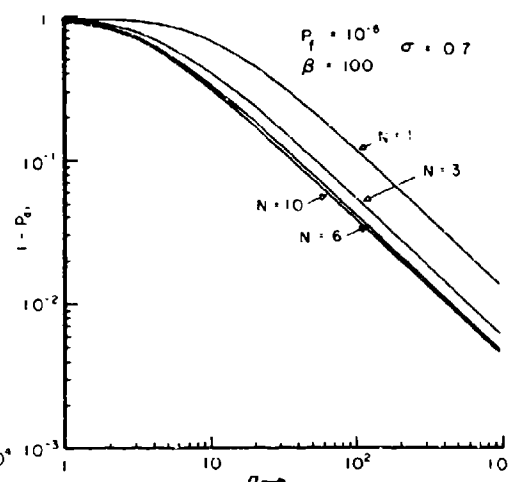


Figure 28. Probability of Detection (Swerling 1) for  $P_f = 10^{-6}$ ,  $\beta = 100$ ,  $\sigma = 0.7$

It is interesting to note from Figures 19-28 that unless  $\beta > 10$ ,  $P_{d1}$  is essentially independent of  $N$ . This is quite evident from physical reasoning because for small noise-to-clutter ratios neither the target nor the clutter-plus-noise fluctuate from pulse-to-pulse. Therefore, summing  $N$ -pulses cannot offer any advantage. This is also evident from (41) and (38). From (38) we have that for  $Y_o$  large

$$Y_o = \frac{H(P_f)N}{\beta} \quad (42)$$

where  $H$  is a function of  $P_f$ . If we use this result in (41) we obtain

$$P_{d1} \approx \exp \left[ -\frac{Y_o}{N\alpha} \right] = \exp \left[ -\frac{H(P_f)}{\alpha\beta} \right] \quad (43)$$

which is clearly independent of  $N$ . For large values of  $\beta$ , the results in (42) and (43) are no longer appropriate because then  $Y_o$  is no longer large, as is required for (42) to be valid.

## 5. DISCUSSION

The results we have presented in Sections 2-4 are strictly valid for a receiver which consists of a square-law detector and integrator. However, most systems operating in an environment where clutter is a consideration are likely to employ an MTI (moving target indicator) to reduce clutter. When an MTI is used our results are only approximately valid, because the noise\* samples are then not statistically independent from pulse-to-pulse, as we have assumed. (This statement applies to the target-plus-noise for a Swerling-2 target.) In order to see this, we consider a single stage MTI. Let  $n_{i-1}$  be the noise present at the input to the MTI at time  $(i-1)\tau$ ,  $n_i$  be the noise at time  $i\tau$ , and  $n_{i+1}$  be the input noise at time  $(i+1)\tau$ . Then the MTI noise output  $\tilde{n}_i$  at time  $i\tau$  is  $\tilde{n}_i = n_{i-1} - n_i$  and the output  $\tilde{n}_{i+1}$  at time  $(i+1)\tau$  is  $\tilde{n}_{i+1} = n_i - n_{i+1}$ . Therefore, even though  $n_{i-1}$ ,  $n_i$  and  $n_{i+1}$  are statistically independent,  $\tilde{n}_i$  and  $\tilde{n}_{i+1}$  are not, because  $\langle \tilde{n}_i \tilde{n}_{i+1} \rangle = \langle (n_{i-1} - n_i)(n_i - n_{i+1}) \rangle = -\langle n_i^2 \rangle \neq 0$ . Consequently, the noise samples at the output of the MTI are partially correlated from pulse-to-pulse. Thus if  $N_0$  of these pulses are integrated, the correct probability of detection will be somewhere between our answers\*\* in Figures 7-28 for  $N = 1$  (complete correlation of all  $N_0$  pulses) and  $N = N_0$  (complete decorrelation). For a single stage MTI, the pulse-to-pulse correlation coefficient is  $1/2$ , for a two stage MTI the correlation coefficient is  $2/3$ , etc. This suggests that the  $N = 1$  results in Figures 7-28 will be a reasonable approximation when a multistage MTI is used, even if  $N$ -pulses are integrated following the MTI.

\*Note that this will not be a problem with the clutter samples because the clutter samples have been assumed to be completely correlated from pulse-to-pulse, and the MTI does not change this. The clutter statistics from scan-to-scan are of course still log-normal.

\*\*The value of the clutter level which would be used in calculating  $\beta$  is the residual clutter level present at the MTI output terminals.



# BEST AVAILABLE COPY

## References

1. Marcum, J., and Swerling, P. (1960) Studies of target detection by pulsed radar, IRE Trans. on Inform Theory TI-6:2.
2. Trunk, G., and George, S. (1970) Detection of targets in non-gaussian sea clutter, IEEE Trans. on Aerospace and Electronic Systems AES-6:620.
3. Schleher, D. (1975) Radar detection in log-normal clutter, IEEE International Radar Conference, IEEE Press (Publication No. 75 CH0938-1 AES), New York.
4. Beckmann, P. (1967) Probability in Communication Engineering, Harcourt, Brace and World, New York.
5. Erdelyi, A., et al (1954) Tables of Integral Transform (Bateman Manuscript Project), McGraw-Hill, New York.
6. Berkowitz, R. (1965) Modern Radar, Wiley, New York.
7. Trunk, G. (1971) Further results on the detection of targets in non-gaussian sea clutter, IEEE Trans. on Aerospace and Electronic Systems AES-7:553.

BEST AVAILABLE COPY

## Appendix A

### Probability Density for a Constant Target

Here we give the probability density for the envelope squared of the sum of  $N$ -independent samples from a constant target immersed in Rayleigh noise which varies from pulse-to-pulse and log-normal clutter which varies from scan-to-scan. For  $Y \geq 0$ , the result is

$$P(Y) = \frac{e^{-Y}}{(2\pi)^{3/2} \sigma} \int_0^\infty d\xi e^{-\xi} G_N(\xi, Y) \int_0^\infty d\phi \exp \left\{ -\frac{\ln^2 [\beta(2\xi - 2^{3/2} a \xi^{1/2} + a^2)N^{-1}]}{8\sigma^2} \right\} \quad (A1)$$

$$\frac{2\xi - 2^{3/2} a \xi^{1/2} + a^2}{8\sigma^2}$$

where  $a = N^{1/2} C / \sigma_n$ ,  $C$  is the (constant) target voltage and  $\beta$ ,  $Y$ ,  $G_N$  etc. are as defined previously.

## Appendix B

### Derivation of Equation (38)

If we let  $\eta = Y/Y_0$  and  $\xi = Y_0 t$ , we can rewrite (35) as

$$P_f = \frac{Y_0}{2(2\pi)^{1/2}\sigma} \int_1^\infty d\eta \int_0^\infty \frac{dt}{t} \left(\frac{\eta}{t}\right)^{(N-1)/2} I_{N-1} [2Y_0(\eta t)^{1/2}] \exp \left\{ -Y_0(\eta + t) - \frac{1}{8\sigma^2} \ln^2 \left( \frac{2\beta Y_0}{N} t \right) \right\} . \quad (B1)$$

For  $Y_0 \gg 1$ , we can use the asymptotic expansion for  $I_{N-1}(Z)$ . If this is done and we also make the substitution  $t = x^2$  and  $\eta = v^2$ , we can rewrite (B1) as

$$P_f = \frac{(2Y_0)^{1/2}}{2\pi\sigma} \int_1^\infty v^{1/2} dv \int_0^\infty \frac{dx}{x^{3/2}} \left(\frac{v}{x}\right)^{N-1} \exp \left[ -Y_0(x - v)^2 - \frac{1}{8\sigma^2} \ln^2 \left( \frac{2\beta Y_0}{N} x^2 \right) \right] . \quad (B2)$$

For  $Y_0 \rightarrow \infty$  it is clear that the integrand of the  $x$  integral is sharply peaked about  $x = v$ , because of the term  $\exp [-Y_0(x - v)^2]$ . Therefore, we can set  $x = v$  in the entire  $x$  integrand, except for  $\exp [-Y_0(x - v)^2]$  to get

$$P_f \approx \frac{(2Y_0)^{1/2}}{2\pi\sigma} \int_1^\infty \frac{dv}{v} \exp \left\{ -\frac{1}{2\sigma^2} \ln^2 \left[ \left( \frac{2\beta Y_0}{N} \right)^{1/2} v \right] \right\} \int_{-\infty}^\infty dz e^{-Y_0 z^2} \quad (B3)$$

where in the last integral in (B3) we have replaced  $x - v$  by  $z$  and extended the range of integration on  $z$  to the entire real line. If we perform the  $z$  integral and then let  $u = (2)^{-1/2} \sigma^{-1} \ln [v(2\beta Y_0/N)^{1/2}]$  we get

$$P_f \approx \frac{1}{(\pi)^{1/2}} \int_p^\infty e^{-u^2} du \quad (B4)$$

where  $p = (8\sigma^2)^{-1/2} \ln (2\beta Y_0/N)$ . Equation (38) follows immediately from (B4).

## Appendix C

### Derivation of Equation (40)

For large  $\alpha$ , it is convenient to rewrite (37) as

$$P_{d2} = 1 - \frac{1}{2\sigma(2\pi)^{1/2}} \int_0^{\frac{Y_0}{1+\alpha}} e^{-Y} dY \int_0^\infty \frac{d\xi}{\xi} \left(\frac{Y}{\xi}\right)^{(N-1)/2} I_{N-1}[2(Y\xi)^{1/2}] \exp \left[ -\xi - \frac{1}{8\sigma^2} \ln^2 \left( \frac{2\alpha\beta\xi}{N} \right) \right] \quad (C1)$$

As  $\alpha \rightarrow \infty$ , it is clear that most of the contribution to the integral comes from  $\xi$  near zero. Therefore, we may expand  $I_{N-1}(\dots)$  in a Taylor series about  $\xi = 0$  to obtain

$$P_{d2} \approx 1 - \frac{1}{2\sigma(2\pi)^{1/2}} \int_0^{\frac{Y_0}{1+\alpha}} \frac{dY e^{-Y} Y^{N-1}}{(N-1)!} \int_0^\infty \frac{d\xi}{\xi} \exp \left[ -\frac{1}{8\sigma^2} \ln^2 \left( \frac{2\alpha\beta\xi}{N} \right) \right] . \quad (C2)$$

If we recall that

$$\frac{1}{2(2\pi)^{1/2}\sigma} \int_0^\infty \frac{d\xi}{\xi} \exp \left[ -\frac{1}{8\sigma^2} \ln^2(A\xi) \right] = 1$$

we see that (C2) becomes

$$P_{d2} \simeq 1 - \int_0^{\frac{Y_0}{1+\sigma}} \frac{dY e^{-Y} Y^{N-1}}{(N-1)!} \quad (C3)$$

Finally, if we use form 5 on p. 134 of Ref. 1, we can evaluate the integral in (C3) to yield (40).

- 
1. Erdelyi, A., et al (1954) Tables of Integral Transform (Bateman Manuscript Project), McGraw-Hill, New York.

# METRIC SYSTEM

## BASE UNITS:

Quantity	Unit	SI Symbol	Formula
length	metre	m	...
mass	kilogram	kg	...
time	second	s	...
electric current	ampere	A	...
thermodynamic temperature	kelvin	K	...
amount of substance	mole	mol	...
luminous intensity	candela	cd	...

## SUPPLEMENTARY UNITS:

plane angle	radian	rad	...
solid angle	steradian	sr	...

## DERIVED UNITS:

Acceleration	metre per second squared	...	m/s <sup>2</sup>
activity (of a radioactive source)	disintegration per second	...	(disintegration)/s
angular acceleration	radian per second squared	...	rad/s <sup>2</sup>
angular velocity	radian per second	...	rad/s
area	square metre	...	m <sup>2</sup>
density	kilogram per cubic metre	...	kg/m <sup>3</sup>
electric capacitance	farad	F	A <sup>2</sup> /V
electrical conductance	siemens	S	A/V
electric field strength	volt per metre	...	V/m
electric inductance	henry	H	V <sup>2</sup> /A
electric potential difference	volt	V	W/A
electric resistance	ohm	...	V/A
electromotive force	volt	V	W/A
energy	joule	J	N <sup>2</sup> /m
entropy	joule per kelvin	...	J/K
force	newton	N	kg <sup>2</sup> /m/s <sup>2</sup>
frequency	hertz	Hz	(cycle)/s
illuminance	lux	lx	lm/m <sup>2</sup>
luminance	candela per square metre	...	cd/m <sup>2</sup>
luminous flux	lumen	lm	cd <sup>2</sup> /sr
magnetic field strength	ampere per metre	...	A/m
magnetic flux	weber	Wb	V <sup>2</sup> /s
magnetic flux density	tesla	T	Wb/m <sup>2</sup>
magnetomotive force	ampere	A	...
power	watt	W	J/s
pressure	pascal	Pa	N/m <sup>2</sup>
quantity of electricity	coulomb	C	A <sup>2</sup> /s
quantity of heat	joule	J	N <sup>2</sup> /m
radiant intensity	watt per steradian	...	W/sr
specific heat	joule per kilogram-kelvin	...	J/kg <sup>2</sup> -K
stress	pascal	Pa	N/m <sup>2</sup>
thermal conductivity	watt per metre-kelvin	...	W/m <sup>2</sup> -K
velocity	metre per second	...	m/s
viscosity, dynamic	pascal-second	...	Pa <sup>2</sup> /s
viscosity, kinematic	square metre per second	...	m <sup>2</sup> /s
voltage	volt	V	W/A
volume	cubic metre	...	m <sup>3</sup>
wavenumber	reciprocal metre	...	(wave)/m
work	joule	J	N <sup>2</sup> /m

## SI PREFIXES:

Multiplication Factors	Prefix	SI Symbol
1 000 000 000 000 = 10 <sup>12</sup>	tera	T
1 000 000 000 = 10 <sup>9</sup>	giga	G
1 000 000 = 10 <sup>6</sup>	mega	M
1 000 = 10 <sup>3</sup>	kilo	k
100 = 10 <sup>2</sup>	hecto*	h
10 = 10 <sup>1</sup>	deka*	da
0.1 = 10 <sup>-1</sup>	deci*	d
0.01 = 10 <sup>-2</sup>	centi*	c
0.001 = 10 <sup>-3</sup>	milli	m
0.000 001 = 10 <sup>-6</sup>	micro	μ
0.000 000 001 = 10 <sup>-9</sup>	nano	n
0.000 000 000 001 = 10 <sup>-12</sup>	pico	p
0.000 000 000 000 001 = 10 <sup>-15</sup>	femto	f
0.000 000 000 000 000 001 = 10 <sup>-18</sup>	atto	a

\* To be avoided where possible.